Complex Number Formulation and Convex Relaxations for Aircraft Conflict Resolution

David Rey and Hassan Hijazi

Abstract—We present a novel complex number formulation along with tight convex relaxations for the aircraft conflict resolution problem. Our approach combines both speed and heading control and provides global optimality guarantees despite non-convexities in the feasible region. As a side result, we present a new characterization of the conflict separation condition in the form of disjunctive linear constraints. Our formulation features one binary variable per pair of aircraft, is free of trigonometric functions, and captures the non-convexity in a set of quadratic concave constraints. Using our approach, we are able to close a number of open instances and reduce computational time by up to two orders of magnitude on standard instances.

I. INTRODUCTION

The steady increase in air travel demand continuously exposes air traffic networks to surges in congestion which affects passenger delay and operating costs [1]. Air Traffic Management (ATM) initiatives have been launched in major air traffic networks (Western Europe [2], United States [3]) in an effort to absorb this stress while maintaining a high level of safety as well as reducing delays and environmental footprint in aviation. Safety plays a critical role in ATM due to the high stakes involved in aircraft operations. The safety of flights is ensured by Air Traffic Control (ATC) services which are in charge of monitoring aircraft trajectories and maintaining minimum separation distances between aircraft [4]. Current air separation standards issued by the International Civil Aviation Organization (ICAO) require that aircraft be separated by at least 5 NM¹ horizontally and 1000 ft vertically [5] and two aircraft violating these rules are said to be in *conflict*. In this paper, we present a novel Conflict Detection and Resolution (CDR) algorithm based on speed and heading control for en-route traffic.

During en-route operations, which represents the major phase of a flight, vertical separation is typically ensured as long as aircraft maintain their assigned flight level. In turn, horizontal separation standards dictate that precautions be taken at flight trajectory intersections—generally represented by a waypoint—where most potential air conflicts occur. To anticipate a potential loss of separation between two or more aircraft, it is necessary to predict aircraft trajectories over a look-ahead period and track their relative distance. In current ATC operations, predicted air conflicts are handled by flight trajectory maneuvers which combine heading angle deviation and altitude change. These separation maneuvers have been widely used since the emergence of ATC operations since they can be represented by radar vectors which can be easily processed by air traffic controllers [6]. From a mathematical standpoint, altitude change maneuvers can be easily modeled using discrete decision variables since aircraft must travel at specific flight levels which are separated *a priori*. In turn, horizontal separation maneuvers often require more complex formulations, especially when heading control is allowed. Hence, in this paper, we focus on the horizontal aircraft conflict resolution problem, *i.e.*, we propose solution methods for collision avoidance in the 2-dimensional plane.

II. STATE OF THE ART

The aircraft conflict resolution problem is traditionally represented as an optimization problem in which the objective is to find conflict-free trajectories for all aircraft flying in a given region of airspace. A comprehensive review of the literature on CDR algorithms up to the 21st century can be found in [7]. During the last couple of decades, there has been a considerable amount of research focusing on global optimization approaches for aircraft conflict resolution whereas prior efforts focused on scalable heuristic methods. Since we propose a global optimization approach for the aircraft conflict resolution problem, we next focus on reviewing the literature on exact methods.

The first exact approaches for conflict resolution are due to [8] and [9]. In [8], the authors propose a Mixed-Integer Linear Program (MILP) to find conflict-free aircraft trajectories in the horizontal space. Aircraft dynamics are approximated and separation constraints are verified at discrete time steps. An optimal control formulation with speed and heading maneuvers is proposed and solved on instances with up to 4 aircraft. In [9], two horizontal conflict resolution problems are solved: a first problem is solved with speed control only and a second with heading control.

Subsequent efforts have focused on speed control or speed and altitude control approaches which can be modeled as MILPs. In [10], the authors present a MILP for speed and altitude control based on a disjunctive linear separation constraint. This separation condition is also used in [11] where the authors formulate the problem as a MILP where speed control is the only separation maneuver. Since all conflicts may not be resolved using speed control only, two objective functions that aim to maximize the number of conflicts resolved and minimize the total duration of conflicts are proposed.

D. Rey is with School of Civil and Environmental Engineering, UNSW Sydney, 2052, NSW, Australia d.rey@unsw.edu.au

H. Hijazi is with the Australian National University and Data61-CSIRO, 2601 ACT, Canberra, Australia hassan.hijazi@anu.edu.au

¹Nautical Mile—1 NM = 1852 m.

The crossing time separation condition is also used in [12] which proposes a space-discretized MILP formulation involving speed and heading controls and incorporating constraints on aircraft acceleration and yaw rate. In contrast to most other approaches, the heading control maneuvers consists of two actions: a first heading change to deviate and subsequent ones to recover the initial heading.

Several papers have built on the shadow separation constraints introduced in [9] to derive formulations for 3D problem involving speed and altitude control [13], heading control [14] and all three types of maneuvers [15]. In all these papers, the authors minimize a criterion representing the deviation to aircraft initial trajectories. In [13], the problem is represented as a MILP and improvements on the original formulation are proposed.

In [14], a Mixed-Integer Non-Linear Program (MINLP) is proposed to solve the horizontal aircraft collision avoidance problem based on shadow separation constraints. These constraints are expressed using trigonometric functions to represent heading variations.

Recently, in [15], the authors proposed an exact optimization approach combining speed, heading and altitude controls. The proposed formulation is essentially a non-convex MINLP where all three types of separation maneuvers are allowed. The authors also consider a 2D variant of their problem in which only horizontal maneuvers (speed and heading control) are allowed. The proposed MINLP is solved using Minotaur [16].

Let us emphasize that, in [13], [14], [15], the authors point out the existence of past conflicts in their formulations without providing a comprehensive method to handle these. In particular, if heading control is allowed, initially diverging aircraft (before optimization) can eventually converge (after optimization).

Alternative separation conditions derived from aircraft pairs time of minimal distance were recently proposed in [17], [18] and formulated using MINLPs. Using the time of minimal separation, aircraft divergence can be modeled as a separation maneuver. In [18], the authors address the horizontal aircraft conflict resolution with speed and heading control and propose a method to sequentially apply speed then heading controls. The objective is to minimize the l_2 -norm of heading controls and the problems are solved with Couenne [19].

This review highlights the difficulty to solve the aircraft conflict resolution problem with speed and heading control. Exact approaches are penalized by the non-convexity of trigonometric functions involved in defining the separation conditions. In turn, discretised approaches either use upper bounds on aircraft minimal crossing times to guarantee conflict-free trajectories or consider only a finite number of alternative trajectories, thus potentially ignoring conflict-free solutions with better objective function values. In this paper, we present a new formulation for aircraft separation based on a complex number representation of velocity control. We then introduce convex relaxations in the form of Mixed-Integer Quadratic Programs (MIQPs) and a Mixed-Integer Quadratically-Constrained Programs (MIQCPs). We show that these convex relaxations are likely to produce global optimal solutions, i.e., the relaxations are usually tight. Numerical results highlight the efficiency of the proposed approach when compared to state-of-the-art methods on classical benchmark problems.

III. AIRCRAFT SEPARATION CONDITION

In this section, we present a new formulation for the aircraft separation condition which relies on aircraft relative motion. Let us consider a set A of aircraft in a given air sector, all at the same flight level. Let $p_i(t) = [x_i(t), y_i(t)]^{\mathsf{T}}$ be the vector representing the position of flight i at time t. The relative position of aircraft i and j at time t can be represented as $p_{ij}(t) = p_i(t) - p_j(t)$. Let d be the horizontal separation norm, the two aircraft are separated if and only if:

$$\|\boldsymbol{p}_{ij}(t)\| \ge d, \forall t \ge 0 \tag{1}$$

Let $v_{ij} = [v_{ij,x}, v_{ij,y}]^{\mathsf{T}}$ be the relative velocity vector of iand j, *i.e.*, $v_{ij,x} = v_{i,x} - v_{j,x}$ and $v_{ij,y} = v_{i,y} - v_{j,y}$, and let $\hat{p}_{ij} = [\hat{x}_{ij}, \hat{y}_{ij}]^{\mathsf{T}}$ be their relative initial positions. Assuming that uniform motion laws apply, $p_{ij}(t)$ can be expressed as: $p_{ij}(t) = \hat{p}_{ij} + v_{ij}t$.

For each aircraft $i \in A$, we denote \hat{v}_i its initial speed and $\hat{\theta}_i$ its initial heading. Let q_i be the speed variation rate $(q_i = 1 \text{ means no deviation})$ and let θ_j be the heading deviation angle $(\theta_i = 0 \text{ means no deviation})$: q_i and θ_i are the main speed and heading control variables for $i \in A$, respectively. Aircraft velocity components are

$$v_{i,x} = q_i \hat{v}_i \cos(\theta_i + \hat{\theta}_i)$$
 and $v_{i,y} = q_i \hat{v}_i \sin(\theta_i + \hat{\theta}_i)$.

Aircraft relative velocity vector components can then be written as

$$v_{ij,x} = q_i \hat{v}_i \cos(\theta_i + \hat{\theta}_i) - q_j \hat{v}_j \cos(\theta_j + \hat{\theta}_j)$$
(2)

$$v_{ij,y} = q_i \hat{v}_i \sin(\theta_i + \hat{\theta}_i) - q_j \hat{v}_j \sin(\theta_j + \hat{\theta}_j)$$
(3)

Modeling aircraft separation can be achieved by determining the time of minimum separation based on aircraft relative motion [20], [17]. Squaring Equation (1) we obtain the separation condition

$$f_{ij}(t) \equiv \|\boldsymbol{v}_{ij}\|^2 t^2 + 2\hat{\boldsymbol{p}}_{ij} \cdot \boldsymbol{v}_{ij} t + \|\hat{\boldsymbol{p}}_{ij}\|^2 - d^2 \ge 0 \quad (4)$$

where \cdot is the inner product in the Euclidean space. From Equation (4), $f_{ij}(t)$ is a 2nd order convex polynomial in t which is minimal when its derivative vanishes. Let t_{ij}^m be the time at which $f_{ij}(t)$ is minimal

$$f'_{ij}(t) = 0 \quad \Leftrightarrow \quad t^m_{ij} = \frac{-\hat{\boldsymbol{p}}_{ij} \cdot \boldsymbol{v}_{ij}}{\|\boldsymbol{v}_{ij}\|^2} \tag{5}$$

Note that the sign of the inner product $\hat{p}_{ij} \cdot v_{ij}$ indicates aircraft convergence/divergence, formally we can state that,

$$\hat{\boldsymbol{p}}_{ij} \cdot \boldsymbol{v}_{ij} > 0 \Leftrightarrow t^m_{ij} < 0 \tag{6}$$

which indicates that aircraft i and j are diverging. Modeling aircraft divergence is critical if heading control maneuvers

are allowed since a pair of initially diverging aircraft (before optimization) may converge (after optimization).

Substituting t_{ij}^m in $f_{ij}(t)$, the separation condition (4) can be simplified to $f_{ij}(t_{ij}^m) \ge 0$, which does not depend on t anymore. Furthermore, multiplying both sides by $\|\boldsymbol{v}_{ij}\|^2$ gives the following separation condition

$$g_{ij}(\boldsymbol{v}_{ij}) = \|\boldsymbol{v}_{ij}\|^2 f_{ij}(t_{ij}^m) = \|\boldsymbol{v}_{ij}\|^2 (\|\hat{\boldsymbol{p}}_{ij}\|^2 - d^2) - (\hat{\boldsymbol{p}}_{ij} \cdot \boldsymbol{v}_{ij})^2 \ge 0$$
(7)

For clarity of presentation, we will drop the ij subscript in the remainder of this section. In scalar form, the separation condition (7) can be written as a function of aircraft relative velocity:

$$g(v_x, v_y) = v_x^2(\hat{y}^2 - d^2) + v_y^2(\hat{x}^2 - d^2) - v_x v_y(2\hat{x}\hat{y}) \ge 0 \quad (8)$$

The separation constraint (7) provides a sufficient condition for aircraft separation but ignores the temporal dimension of the problem as it cannot differentiate between past and future conflicts. In particular, diverging aircraft do not have to satisfy these constraints as they incur no risk of future conflicts (assuming they are initially separated).

We next build on (8) and derive a new formulation of the pairwise separation condition. Our approach is based on the observation that the non-convex region corresponding to feasible velocity controls can be represented as the union of two disjoint convex sub-regions.

Note that the function g on the left hand side of (8) is a two-dimensional quadratic function. Thus, the feasible region corresponding to the equation $g(v_x, v_y) = 0$ can be described by two linear equations. These equations are characterised by solving the equation $g(v_x, v_y) = 0$ treating v_y or v_x as a constant. The discriminants of the resulting uni-dimensional quadratic functions are

$$\begin{cases} \Delta_{v_x} = 4d^2 v_y^2 (\hat{x}^2 + \hat{y}^2 - d^2) \\ \frac{1}{2} (\hat{x}^2 + \hat{y}^2 - d^2) \end{cases}$$
(9)

$$\begin{pmatrix} \Delta_{v_y} = 4d^2 v_x^2 (\hat{x}^2 + \hat{y}^2 - d^2) & (10) \\ \vdots & \vdots \\ \end{pmatrix}$$

Hence the equation admits real roots if $\hat{x}^2 + \hat{y}^2 - d^2 \ge 0$, which is always true since *i* and *j* are assumed to be initially separated.

Given the discriminants defined in (9) and (10), points satisfying $g(v_x, v_y) = 0$ must satisfy the following set of linear equations,

$$(\hat{y}^2 - d^2)v_x - \left(\hat{x}\hat{y} + d\sqrt{\hat{x}^2 + \hat{y}^2 - d^2}\right)v_y = 0$$
(11)

$$(\hat{y}^2 - d^2)v_x - \left(\hat{x}\hat{y} - d\sqrt{\hat{x}^2 + \hat{y}^2 - d^2}\right)v_y = 0$$
(12)

$$(\hat{x}^2 - d^2)v_y - \left(\hat{x}\hat{y} - d\sqrt{\hat{x}^2 + \hat{y}^2 - d^2}\right)v_x = 0$$
(13)

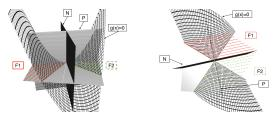
$$(\hat{x}^2 - d^2)v_y - \left(\hat{x}\hat{y} + d\sqrt{\hat{x}^2 + \hat{y}^2 - d^2}\right)v_x = 0$$
(14)

Let us emphasise that if all coefficients in (11)-(14) are non-zero, then (11) is identical to (13) and (12) is identical to (14). Observe that,

$$\begin{split} \hat{x}\hat{y} \pm d\sqrt{\hat{x}^2 + \hat{y}^2 - d^2} &= 0 \\ \Rightarrow & d^2(\hat{x}^2 + \hat{y}^2 - d^2)^2 = \hat{x}^2\hat{y}^2 \\ \Leftrightarrow & \hat{x}^2\hat{y}^2 - d^2(\hat{x}^2 + \hat{y}^2 - d^2)^2 = 0 \\ \Leftrightarrow & (\hat{x}^2 - d^2)(\hat{y}^2 - d^2) = 0 \end{split}$$

Hence the coefficients in (11)-(14) are non-zero if $|\hat{x}| \neq d$ and $|\hat{y}| \neq d$. If one coefficient is zero, e.g., let $\hat{x} \ge 0$ and $\hat{y} = -d$, then (11) becomes a tautology while (13) simplifies to $v_y = 0$.

Equations (11)-(14) define two lines in the plane (v_x, v_y) and the sign of $g(v_x, v_y)$ depends on these linear equations. An Example of the non-convex region defined by the inequality $g(v_x, v_y) \ge 0$ is depicted in Figure 1.



(a) Side-view of the feasible region (b) Upper-view of the feasible region

Fig. 1. Different angles on the feasible region in the plane (v_x, v_y) . Note that points behind the hyperplane (P) are feasible (past conflicts) and (N) splits the feasible region into two symmetric convex sub-regions denoted F1 and F2.

Consider the plane equation

$$v_x \hat{x} + v_y \hat{y} = 0 \tag{P}$$

induced by the dot product $\hat{p}_{ij} \cdot v_{ij}$ and indicating convergence/divergence. This plane splits the space (v_x, v_y) in two half-spaces, one of which represents diverging trajectories. Any point in this half-space corresponds to diverging trajectories and is thus feasible. The remaining half-space can be split into two symmetric sub-spaces using the plane normal to $v_x \hat{x} + v_y \hat{y} = 0$, defined as,

$$v_y \hat{x} - v_x \hat{y} = 0 \tag{N}$$

as shown in Proposition 1.

Proposition 1: The normal plane (N) is the bisector of the angle formed by the two lines representing the solutions of $g(v_x, v_y) = 0$.

Proof: Note that the slope of the plane defined by (N) is $\frac{y}{\hat{x}}$. Without any loss of generality, assume that $|\hat{x}| > d$ (the case $|\hat{x}| \leq d$ can be treated similarly by working in the rotated plane used to handle pathological cases).

Let

$$r_1 = \frac{\hat{x}\hat{y} + d\sqrt{\hat{x}^2 + \hat{y}^2 - d^2}}{\hat{x}^2 - d^2} \text{ and } r_2 = \frac{\hat{x}\hat{y} - d\sqrt{\hat{x}^2 + \hat{y}^2 - d^2}}{\hat{x}^2 - d^2}$$

be the slopes of the lines defined by (13) and (14). The angle of the bisector of these lines is $\mu = \frac{1}{2}(\arctan r_1 + \arctan r_2)$ and its slope is:

$$\tan(\mu) = \tan\left(\frac{1}{2}\left(\arctan(r_1) + \arctan(r_2)\right)\right)$$
$$= \tan\left(\frac{1}{2}\left(\arctan\left(\frac{r_1 + r_2}{1 - r_1 r_2}\right)\right)\right)$$

If $r_1r_2 = 1$, recall that $\lim_{X \to \pm \infty} \arctan(X) = \pm \pi/2$, thus $\tan(\mu) = \tan(\frac{1}{2}\frac{\pm \pi}{2}) = \tan(\pm \pi/4) = \pm 1$. In addition, $r_1r_2 = \frac{\hat{y}^2 - d^2}{\hat{x}^2 - d^2}$, hence $r_1r_2 = 1 \Leftrightarrow \hat{y}^2 = \hat{x}^2$ and the slope of the plane defined by (N) is ± 1 . Assume now $r_1r_2 \neq 1$, using the half-angle formula, $\tan(\mu)$ can be written as:

$$\tan(\mu) = \frac{\sqrt{1 + \left(\frac{r_1 + r_2}{1 - r_1 r_2}\right)^2 - 1}}{\left(\frac{r_1 + r_2}{1 - r_1 r_2}\right)}$$

Since $\frac{r_1+r_2}{1-r_1r_2} = \frac{2\hat{x}\hat{y}}{\hat{x}^2-\hat{y}^2}$, this gives: $\tan(\mu) = \frac{\sqrt{(\hat{x}^2 - \hat{y}^2)^2 + 4\hat{x}\hat{y}} - (\hat{x}^2 - \hat{y}^2)}{2\hat{x}\hat{y}} = \frac{\hat{y}}{\hat{x}}$

This property provides an intuitive approach to partition the feasible region. Given a binary variable $z \in \{0, 1\}$, let us consider the following disjunction,

$$\{z = 1, v_y \hat{x} - v_x \hat{y} \leq 0\} \lor \{z = 0, v_y \hat{x} - v_x \hat{y} \geq 0\}.$$

This disjunction models the crossing order of aircrafts at the intersection point of their trajectories.

Let us emphasize that the feasible region defined by the separation constraint (8) can be reduced to two on/off linear inequalities based on (11)-(14). Depending on the sign of constants \hat{x} and \hat{y} , (8) can only be satisfied on one side of the lines defined by the system of linear equations. Given the disjunction above, the feasible region can be split into two symmetrical polyhedra defined by the lines corresponding to the roots of (8). This is illustrated in Figure 1. We next present a new formulation to link relative velocity variables to aircraft control variables.

IV. COMPLEX NUMBER FORMULATION

Aircraft motion can be represented by the vector $v_i = [v_{i,x}, v_{i,y}]^{\mathsf{T}}$ where $v_{i,x} = q_i \hat{v}_i \cos(\theta_i + \hat{\theta}_i)$ and $v_{i,y} = q_i \hat{v}_i \sin(\theta_i + \hat{\theta}_i)$. Recall that the decision variables are the acceleration rate q_i and the heading angle deviation from the initial heading θ_i . We propose to isolate these decision variables using trigonometric identities:

$$\begin{aligned} v_{i,x} &= q_i \hat{v}_i \cos(\theta_i) \cos(\hat{\theta}_i) - q_i \hat{v}_i \sin(\theta_i) \sin(\hat{\theta}_i) \\ v_{i,y} &= q_i \hat{v}_i \sin(\theta_i) \cos(\hat{\theta}_i) - q_i \hat{v}_i \cos(\theta_i) \sin(\hat{\theta}_i) \end{aligned}$$

This representation admits a natural formulation where the velocity control actions are represented as a complex number:

$$V_i = q_i(\cos(\theta_i) + i\sin(\theta_i))$$

In rectangular form, let $V_i = \delta_{i,x} + \delta_{i,y}i$, we have:

$$\delta_{i,x} = q_i \cos(\theta_i)$$

$$\delta_{i,y} = q_i \sin(\theta_i)$$

The magnitude of V_i is then $|V_i| = \sqrt{\delta_{i,x}^2 + \delta_{i,y}^2} = q_i$ and its argument $\arg(V_i) = \arctan 2(\delta_{i,y}, \delta_{i,x}) = \theta_i$. This approach is inspired by complex number formulations for the optimal power flow problem in power systems [21], [22].

A common objective function for aircraft conflict resolution is to minimize the deviation with respect to initial trajectories [9], [18], [15]. This can be achieved by minimizing the norm of both $(1 - q_i)$ and θ_i . Observe that

 $\delta_{i,y}^2 + (1 - \delta_{i,x})^2 = q_i^2 - 2q_i \cos(\theta_i) + 1$ which is minimal when $\theta_i = 0$ and $q_i = 1$. Hence we propose to minimize the objective function:

minimize
$$\sum_{i \in A} \delta_{i,y}^2 + (1 - \delta_{i,x})^2$$
(15)

For each $i \in A$, let $0 < \underline{q} < \overline{q}$ be bounds on q_i and let $\underline{\theta} < \overline{\theta}$ be bounds on θ_i . We assume that $\underline{\theta} > -\pi/2$ and $\overline{\theta} < \pi/2$. This is reasonable since aircraft heading control range is typically limited to $\pm \pi/6$ due to aircraft dynamics and passenger comfort constraints. This implies bounds on $\delta_{i,x}$ and $\delta_{i,y}$:

$$\underline{q}\cos(\min\{|\underline{\theta}|, |\overline{\theta}|\}) \leqslant \delta_{i,x} \leqslant \overline{q}$$
(16)

$$q\sin(\underline{\theta}) \leqslant \delta_{i,y} \leqslant \overline{q}\sin(\theta) \tag{17}$$

Further, observe that $\delta_{i,y}/\delta_{i,x} = \tan(\theta_i)$ which is smooth between $-\pi/2$ and $\pi/2$ ($\delta_{i,x} > 0$). Hence, the traditional constraints on aircraft control variables q_i and θ_i can be expressed in the rectangular space ($\delta_{i,x}, \delta_{i,y}$) as follows:

$$\underline{q} \leqslant q_i \leqslant \overline{q} \Leftrightarrow \underline{q}^2 \leqslant \delta_{i,x}^2 + \delta_{i,y}^2 \leqslant \overline{q}^2 \tag{18}$$

$$\underline{\theta} \leqslant \theta_i \leqslant \overline{\theta} \Leftrightarrow \delta_{i,x} \tan(\underline{\theta}) \leqslant \delta_{i,y} \leqslant \delta_{i,x} \tan(\overline{\theta})$$
(19)

The aircraft conflict resolution problem with speed and heading controls is summarized in Model 1, hereby referred to as the Complex Number formulation. Indicator constraints are used to formulate the disjunction therein: depending on the implementation framework, these can be directly passed to the solver or a convex hull formulation can be used based on the methods presented in [23], [24], [25].

Model 1 (Complex Number Formulation):

$$\begin{split} & \text{minimize} \sum_{i \in A} \delta_{i,y}^2 + (1 - \delta_{i,x})^2 \\ & \text{subject to} \\ & v_{ij,x} = \delta_{i,x} \hat{v}_i \cos(\hat{\theta}_i) - \delta_{i,y} \hat{v}_i \sin(\hat{\theta}_i) \\ & - \delta_{j,x} \hat{v}_j \cos(\hat{\theta}_j) + \delta_{j,y} \hat{v}_j \sin(\hat{\theta}_j) \\ & - \delta_{j,y} \hat{v}_i \cos(\hat{\theta}_i) - \delta_{i,x} \hat{v}_i \sin(\hat{\theta}_i) \\ & - \delta_{j,y} \hat{v}_j \cos(\hat{\theta}_j) + \delta_{j,x} \hat{v}_j \sin(\hat{\theta}_j) \\ & - \delta_{j,y} \hat{v}_{ij} \cos(\hat{\theta}_j) + \delta_{j,x} \hat{v}_j \sin(\hat{\theta}_j) \\ & v_{ij,y} \hat{x}_{ij} - v_{ij,x} \hat{y}_{ij} \leq 0 \text{ if } z_{ij} = 1 \\ & \forall (i,j) \in P \\ v_{ij,y} \alpha_{ij}^l - v_{ij,x} \beta_{ij}^l \leq 0 \text{ if } z_{ij} = 1 \\ & \forall (i,j) \in P \\ v_{ij,y} \alpha_{ij}^u - v_{ij,x} \beta_{ij}^u \geq 0 \text{ if } z_{ij} = 0 \\ & \forall (i,j) \in P \\ v_{ij,y} \alpha_{ij}^u - v_{ij,x} \beta_{ij}^u \geq 0 \text{ if } z_{ij} = 0 \\ & \forall (i,j) \in P \\ & q^2 \leq \delta_{i,x}^2 + \delta_{i,y}^2 \leq \bar{q}^2 \\ & \forall i \in A \\ & \delta_{i,x} \tan(\underline{\theta}) \leq \delta_{i,y} \leq \delta_{i,x} \tan(\bar{\theta}) \\ & \forall i \in A \\ & \underline{q} \cos(\min\{|\underline{\theta}|, |\bar{\theta}|\}) \leq \delta_{i,x} \leq \bar{q} \\ & \forall i \in A \\ & \overline{q} \sin(\underline{\theta}) \leq \delta_{i,y} \in \mathbb{R}, \ z_{ij} \in \{0,1\} \\ & \forall (i,j) \in P \\ \end{split}$$

Note that coefficients $\alpha_{ij}^l, \beta_{ij}^l$ and $\alpha_{ij}^u, \beta_{ij}^u$ can be preprocessed based on the sign of \hat{x}_{ij} and \hat{y}_{ij} . For implementation details, a fully reproducible model can be found under: https://github.com/ReyHijazi/Conflict_Resolution. This formulation is non-convex due to the concave quadratic constraints involved in the left inequality of (18) and the

disjunction modeled by the binary variable z_{ij} . We next present convex relaxations for this model.

V. CONVEX RELAXATIONS AND SOLUTION ALGORITHM

Non-convexity in the above formulation can be tackled by deriving the convex hull of (18) as described in [21]. Let $\tilde{\delta}_{i,x} \ge 0$ and $\tilde{\delta}_{i,y} \ge 0$ be auxiliary decision variables defined for each $i \in A$ as:

$$q^2 \leqslant \tilde{\delta}_{i,x} + \tilde{\delta}_{i,y} \tag{20}$$

$$\tilde{\delta}_{i,x} \leqslant (1 + \underline{q}\cos(\min\{\underline{\theta},\overline{\theta}\}))\delta_{i,x} - \underline{q}\cos(\min\{\underline{\theta},\overline{\theta}\})$$
(21)

$$\delta_{i,y} \leq q(\sin(\underline{\theta}) + \sin(\overline{\theta}))\delta_{i,y} - q^2\sin(\underline{\theta})\sin(\overline{\theta})$$
(22)

Constraints (20) set a relaxed lower bound on aircraft speed control while Constraints (21) and (22) link variables $\tilde{\delta}_{i,x}$ and $\tilde{\delta}_{i,y}$ to convex envelopes of (18). Substituting the lower bound on $\delta_{i,x}^2 + \delta_{i,y}^2$ in (18) by Constraints (20)-(22) results in a relaxed Mixed-Integer Quadratically Constrained Program (MIQCP) that can be solved by commercial optimization software such as CPLEX [26]—we hereby refer to this relaxation as LB-MIQCP.

The complex number formulation can be further relaxed by entirely omitting Constraints (18). While this relaxation ignores aircraft speed control bounds, the resulting formulation is a Mixed-Integer Quadratic Program (MIQP) for which efficient and scalable algorithms are implemented in optimization software—we hereby refer to this relaxation as LB-MIQP. Observe that LB-MIQP is also a relaxation of LB-MIQCP. Given the objective function, it is expected that both relaxations LB-MIQP and LB-MIQCP often provide solutions that do not violate aircraft speed control bounds. This is due to the objective function in Model 1 aiming at minimizing the deviation to aircraft initial trajectories thus driving q_i away from their bounds.

We use the convex relaxations presented above to solve the horizontal aircraft conflict resolution problem. We first solve LB-MIQP and check if the optimal speed vector q^{\star} violates aircraft speed bounds, i.e., for each aircraft we check if constraints (18) is satisfied. If the solution is bound-violating, we then solve LB-MIQCP and check if the newly obtained q^* violates the lower bound in (18). If the solution is still boundviolating, we introduce a heuristic to efficiently determine a feasible solution by fixing the binary variable vector z^* and solving Model 1 using an interior point method. Note that the Non-Linear Program (NLP) solved in this last step contains only continuous variables and thus provides an upper bound on *OPT*—we hereby refer to this problem as UB-NLP. This solution algorithm is summarized in Algorithm 1. The status of the final solution is either global if the solution of LB-MIQP or LB-MIQCP satisfies Constraints (18); infeas. if one of the two relaxation returns infeasible; local if UB-NLP returns a feasible upper-bound; or nosol. if problem UB-NLP is infeasible.

VI. NUMERICAL RESULTS

In this section, we present numerical results for the horizontal aircraft conflict resolution problem. We test the

Algorithm 1: Solution algorithm for the horizontal aircraft conflict resolution problem

Input: A, θ_0 , v_0 , $q, \overline{q}, \underline{\theta}, \overline{\theta}$
Output: q^* , θ^* , status
$P \leftarrow \{i \in A, j \in A : i < j\}$
$q^{\star}, \theta^{\star}, z^{\star} \leftarrow \text{Solve LB-MIQP}$
if status(LB-MIQP)=infeas. then
status \leftarrow infeas.
return
if $q^* \notin [q, \overline{q}]$ then
$q^{\star}, \bar{\theta}^{\star}, \bar{z}^{\star} \leftarrow$ Solve LB-MIQCP
if status(LB-MIQCP)=infeas. then
status \leftarrow infeas.
return
if $q^{\star} \notin [q, \overline{q}]$ then
$ z \leftarrow z^{\star}$
$q^{\star}, \theta^{\star} \leftarrow $ Solve UB-NLP
if UB-NLP is feasible then
status \leftarrow local
else
status \leftarrow nosol.
else
status ← global
else
status ← global

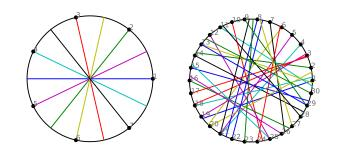


Fig. 2. Illustration of benchmark instances: the CP with 7 aircraft (left) and the RCP with 30 aircraft (right).

performance of the proposed complex number formulation with classical benchmark instances from the literature. We consider two types of instances: the Circle Problem (CP) and the Random Circle Problem (RCP). The CP consists of a set of aircraft uniformly positioned on the circumference of a circle and heading towards its centre. Aircraft speeds are assumed to be identical, hence the problem is highly symmetric. In contrast, the RCP builds on the same framework but aircraft initial speeds and headings are randomly deviated within specified ranges to create random instances with less structure. These benchmarks problems are illustrated in Figure 2 and have been widely used in the field to assess the performance of CDR algorithms [27], [28], [11], [15], [17]. For reproducibility concerns, and for future comparisons, we have uploaded models and instances used here into the public repository: https://github.com/ReyHijazi/Conflict_Resolution.

In all experiments, we use a circle of radius of 200NM. For CP instances, all aircraft have the same initial speed of 500NM/h. For RCP instances, aircraft initial speeds are randomly chosen in the range 486-594NM/h and their initial

headings are deviated from a radial trajectory, (*i.e.*, towards the centre of the circle) by adding a randomly chosen an angle between $-\pi/6$ and $+\pi/6$.

All considered models are implemented using the AMPL modeling language [29] on a personal computer with 8Gb of RAM and an Intel i7 processor at 2.9GHz. The MIQP and MIQCP problems are solved with CPLEX v12.6.3 [26] using default options and a time limit of 300s. The NLP problems are solved with IPOPT with a constraint violation tolerance of $1e^{-9}$ [30]. We use the preprocessing approach presented in [13] to handle pathological cases where a pair of aircraft is near-vertically aligned. Formally, for each pair of aircraft such that $|\hat{x}| \leq d$, we rotate this pair of aircraft by $\pi/2$ counter-clockwise.

A. Experimental Results in the Literature

In [9], heading and speed control formulations are split into two separate MILPs, i.e., speed and heading control maneuvers are not combined, then both models are solved exactly on instances with up to 11 aircraft (speed control) and 17 aircraft (heading control) in a maximum of 15s. In [10], the proposed approach focuses on combined speed and altitude control. An upper bound on aircraft minimal pairwise crossing time is used, hence although solved exactly, the resulting MILP is as a heuristic. Computing time is limited to 10min an no detailed information is available on the optimization performance besides the claim that all problems are solved to optimality within the available time limit. Similarly, in [11], a heuristic MILP is solved for speed control maneuvers only. In [12], the aircraft minimal pairwise crossing time is determined using aircraft initial speeds and a MILP is implemented on the circle problem with only up to 6 aircraft and solved in a few seconds. In addition, grid and trailing scenarios with up to 12 aircraft and 12 conflicts are solved in less than 10s.

In [13], an exact MILP for the speed and altitude control problem is proposed and solved with CPLEX on instances with 20 to 50 aircraft and 5 to 10 flight levels. A total of 25 instances for each combination of number of aircraft and flight levels and statistical results are reported indicating that instances are solved within a few seconds on average. However, the number of initial conflict (before optimization) is not reported, hence making it difficult to evaluate aircraft density in the airspace of interest. In [14], the authors implement an exact approach for the heading control problem and results are reported on the classical Circle Problem benchmark instance with up to 9 aircraft: the non-convex approach exhibits an exponential growth in runtime and requires a few minutes to solve instances with 7 and 8 aircraft, and more than an hour to solve the problem with 9 aircraft. In contrast, the sequential optimization approach is considerably faster with a maximum runtime of 15s and an optimality gap of 2%. Results on random instances are also reported and the non-convex approach is able to solve scenarios with up to 10 in a few minutes while the proposed heuristic is used to solve instances with 25 aircraft and an average number of conflicts of 24.6 in 256s, on average. In

[15], an exact implementation of the combined speed and heading control problem is tested. The authors restrain from reporting results on CP instances with more than 7 aircraft due to scalability issues. Results for larger scenarios are only reported for RCP instances with up to 20 aircraft and an average number of conflicts of 18.6: for this scenario, the horizontal problem is solved in 25-35s based on the selected objective function.

In [18], the authors implement a sequential MINLP approach where the problem is first solved for speed control then remaining conflicts are handled using a heading control optimization. Hence this approach can be seen as a heuristic. Results on the CP instances are reported with up to 6 aircraft, the latter requiring more than 20 minutes. Results on RCP instances are reported on benchmarks with up to 8 aircraft and exhibit runtimes ranging from a few seconds to a few minutes on average. Recently, in [31] the authors propose a minimum weight, maximum cardinality clique MILP formulation in which conflict resolution maneuvers are represented as nodes in a conflict graph. The proposed model is tested on benchmark problems with up to 20 aircraft and 260 maneuvers, including the circle problem. Although all instances are solved within 14s, this remains a maneuverdiscretised method thus falling under heuristic approaches.

B. Our Experimental Results

We test the performance of the proposed solution algorithm 1 on the 17 CP instances with 4 to 20 aircraft. The results for these CP instances are summarized in Table I. In the header, |A| indicates the number of aircraft and n_c indicates the number of initial conflicts n_c (corresponding to the number of conflicts occurring if no control action is taken. The remaining of the table is organized in three subsections corresponding to the three steps of Algorithm 1. In each sub-section, Obj. indicates the objective value, Time indicates the computing time in seconds, Gap indicates the relative optimality gap in % and Status indicates the status returned by Algorithm 1. Further, in subsections LB-MIQP and LB-MIQCP, n_v indicates the number of bound-violating speed constraints (18). Note that a time limit of 300s is imposed for problems LB-MIQP and LB-MIQCP. In subsection UB-NLP, the relative optimality gap is determined using the best of the lower bounds of LB-MIQP and LB-MIQCP.

All CP instances with 4 to 10 aircraft are solved to global optimality within the allocated computing time. Instances with up to 7 aircraft are solved in less than a second while instances with 11 to 19 aircraft are solved to local optimality with an optimality gap of at most 0.22%. This is a substantial improvement compared to existing literature where only results with up to 7 aircraft were reported [15].

To evaluate the performance of the proposed approach on RCP instances, we generated 100 instances for four aircraft set sizes, *i.e.*, 10, 20, 30 and 40 aircraft. The results are presented by reporting, for each aircraft set size, the mean over the 100 instances and the standard deviation in parenthesis. Solution status is reported by indicating the

		LB-MIQP					LB-MIQC	Р				UB-NLP			
A	n_c	Obj.	Time (s)	Gap (%)	Status	n_v	Obj.	Time (s)	Gap (%)	Status	n_v	Obj.	Time (s)	Gap (%)	Status
4	6	0.001250	0.156	0.005	global	-	-	-	-	-	-	-	-	-	-
5	10	0.002273	0.047	0.009	global	-	-	-	-	-	-	-	-	-	-
6	15	0.003619	0.078	0.010	global	-	-	-	-	-	-	-	-	-	-
7	21	0.004747	0.250	0.010	global	-	-	-	-	-	-	-	-	-	-
8	28	0.006921	2.480	0.010	global	-	-	-	-	-	-	-	-	-	-
9	36	0.008622	6.068	0.010	global	-	-	-	-	-	-	-	-	-	-
10	45	0.011099	54.18	0.010	global	-	-	-	-	-	-	-	-	-	-
11	55	0.013776	301.6	0.015	local	-	-	-	-	-	-	-	-	-	-
12	66	0.016763	302.2	0.061	local	-	-	-	-	-	-	-	-	-	-
13	78	0.019583	301.9	0.083	local	-	-	-	-	-	-	-	-	-	-
14	91	0.023149	301.8	0.113	local	-	-	-	-	-	-	-	-	-	-
15	105	0.028053	301.5	0.140	local	-	-	-	-	-	-	-	-	-	-
16	120	0.032872	301.3	0.161	local	-	-	-	-	-	-	-	-	-	-
17	136	0.037093	301.3	0.180	local	-	-	-	-	-	-	-	-	-	-
18	153	0.044903	301.1	0.218	local	-	-	-	-	-	-	-	-	-	-
19	171	0.048754	301.0	0.222	local	-	-	-	-	-	-	-	-	-	-
20	190	0.066015	300.9	0.303	nosol.	2	0.066195	301.1	0.314	nosol.	1	0.067420	0.187	1.818	local

TABLE I Results on the Circle Problem.

distribution of the 100 instances in whole numbers. For formatting purposes, the table is broken into three main rows, each of which corresponds to an optimization problem solved in Algorithm 1.

All 200 10- and 20-aircraft RCP instances are solved to global optimality in one step, *i.e.*, after solving LB-MIQP, in less than a second. The initial conflict density in 30-aircraft RCP instances is more than twice that of 20-aircraft: 76 of them are solved to global optimality in one step while an additional 8 are solved to global optimality in two-steps. All of the remaining 16 instances are solved to local optimality using the proposed heuristic with an average total computing time of 12s and an average optimality gap of 18.6%. 40aircraft instances pose a greater challenge with an average conflict density of 59.3. This leads to an average of 2 boundviolating constraints for LB-MIQP and 1.7 for LB-MIQCP. Consequently, only 18 of the 40-aircraft are solved to global optimality, while 75 are solved to local optimality and 7 out of 100 remain open. Most feasible solutions (boundsatisfying) are found using the heuristic with an average optimality gap of 22% and a standard deviation of 12.2%.

VII. CONCLUSION AND FUTURE WORK

We have introduced a novel formulation for the aircraft conflict resolution problem based on a complex number representation of velocity (speed and heading) control. The new model captures the non-convexity of the feasible region in a set of quadratic and linear on/off constraints. The resulting complex number formulation contains a single disjunction which models the crossing order of aircraft pairs at the intersection point of their trajectories. We introduce convex relaxations for this formulation and present a 3-step solution algorithm for its implementation. The performance of the proposed approach is tested on benchmark problems for conflict resolution. We find that the complex number formulation outperforms existing approaches and is able to solve to global optimality several open instances. Future work will be focused on incorporating altitude control and trajectory prediction uncertainty within the formulation. In addition, multi-action control formulations will be explored to provide a more comprehensive conflict resolution algorithm and enable aircraft to return to their initial headings.

REFERENCES

- Eurocontrol, "Performance review report," Eurocontrol, 96, rue de la Fuse, B-1130 Brussels, Belgium, Tech. Rep., 2011. [Online]. Available: https://www.eurocontrol.int/sites/default/files/ publication/files/prr-2011.pdf
- [2] European Comission and Eurocontrol, "European air traffic management master plan," SESAR, Tech. Rep., 2009.
- [3] Federal Aviation Administration, "FAA's NextGen Implementation Plan," FAA, Tech. Rep., 2011.
- [4] M. Nolan, Fundamentals of Air Traffic Control. Cengage Learning, 2010.
- [5] ICAO, "Rules of the air and air traffic services," International Civil Aviation Organization, Tech. Rep., 1996.
- [6] P. Averty, "Conflict perception by atcs admits doubt but not inconsistency," in 6th USA/Europe Air Traffic Management Research and Development Seminar, Baltimore, USA, 2005.
- [7] J. K. Kuchar and L. C. Yang, "A review of conflict detection and resolution modeling methods," *Intelligent Transportation Systems, IEEE Transactions on*, vol. 1, no. 4, pp. 179–189, 2000.
- [8] A. Richards and J. P. How, "Aircraft trajectory planning with collision avoidance using mixed integer linear programming," in *American Control Conference*, 2002. Proceedings of the 2002, vol. 3. IEEE, 2002, pp. 1936–1941.
- [9] L. Pallottino, E. M. Feron, and A. Bicchi, "Conflict resolution problems for air traffic management systems solved with mixed integer programming," *IEEE transactions on intelligent transportation systems*, vol. 3, no. 1, pp. 3–11, 2002.
- [10] A. Vela, S. Solak, W. Singhose, and J.-P. Clarke, "A mixed integer program for flight-level assignment and speed control for conflict resolution," in *Decision and Control, 2009 held jointly with the 2009 28th Chinese Control Conference. CDC/CCC 2009. Proceedings of the 48th IEEE Conference on*, Dec 2009, pp. 5219–5226.
- [11] D. Rey, C. Rapine, R. Fondacci, and N.-E. El Faouzi, "Subliminal speed control in air traffic management: Optimization and simulation," *Transportation Science*, vol. 50, no. 1, pp. 240–262, 2015.
- [12] J. Omer, "A space-discretized mixed-integer linear model for airconflict resolution with speed and heading maneuvers," *Computers* & *Operations Research*, vol. 58, pp. 75–86, 2015.

		LB-MIQP						
					Status			
A	n_c	Obj.	Time	Gap (%)	global	local	nosol.	n_v
10	3.1 (1.6)	0.000683 (0.001)	0.037 (0.014)	0.004 (0.003)	100	0	0	0.0 (0.0)
20	13.1 (3.5)	0.004097 (0.002)	0.186 (0.048)	0.007 (0.003)	100	0	0	0.0 (0.0)
30	32.9 (5.6)	0.015082 (0.005)	1.881 (1.703)	0.010 (0.001)	76	0	24	0.3 (0.6)
40	59.3 (7.1)	0.037737 (0.012)	33.09 (33.68)	0.010 (0.001)	14	0	86	2.0 (1.6)
		LB-MIQCP						
					Status			
A	n_c	Obj.	Time	Gap (%)	global	local	nosol.	n_v
10	3.1 (1.6)	- (-)	- (-)	- (-)	-	-	-	- (-)
20	13.1 (3.5)	- (-)	- (-)	- (-)	-	-	-	- (-)
30	32.9 (5.6)	0.019750 (0.003)	10.20 (6.160)	0.009 (0.000)	8	0	16	1.1 (0.3
40	59.3 (7.1)	0.040033 (0.010)	202.9 (107.0)	0.013 (0.006)	4	6	76	1.7 (0.8
		UB-NLP						
					Status			
A	n_c	Obj.	Time	Gap (%)	local	nosol.	-	
10	3.1 (1.6)	- (-)	- (-)	- (-)	-	-		
20	13.1 (3.5)	- (-)	- (-)	- (-)	-	-		
30	32.9 (5.6)	0.021132 (0.003)	0.248 (0.040)	18.60 (9.113)	16	0		
40	59.3 (7.1)	0.049286 (0.020)	0.478 (0.076)	22.00 (12.24)	69	7		

TABLE II
RESULTS ON THE RANDOM CIRCLE PROBLEM.

- [13] A. Alonso-Ayuso, L. Escudero, and F. Martín-Campo, "Collision avoidance in air traffic management: A mixed-integer linear optimization approach," *Intelligent Transportation Systems, IEEE Transactions* on, vol. 12, no. 1, pp. 47–57, March 2011.
- [14] A. Alonso-Ayuso, L. F. Escudero, and F. J. Martín-Campo, "Exact and approximate solving of the aircraft collision resolution problem via turn changes," *Transportation Science*, vol. 50, no. 1, pp. 263–274, 2014.
- [15] —, "An exact multi-objective mixed integer nonlinear optimization approach for aircraft conflict resolution," *TOP*, vol. 24, no. 2, pp. 381– 408, 2016.
- [16] S. Leyffer, J. Linderoth, J. Luedtke, A. Mahajan, and T. Munson, "Minotaur," ANL, 2015. [Online]. Available: https://wiki.mcs.anl.gov/ minotaur/index.php/MINOTAUR
- [17] S. Cafieri and D. Rey, "Maximizing the number of conflict-free aircraft using mixed-integer nonlinear programming," *Computers & Operations Research*, vol. 80, pp. 147–158, 2017.
- [18] S. Cafieri and R. Omheni, "Mixed-integer nonlinear programming for aircraft conflict avoidance by sequentially applying velocity and heading angle changes," *European Journal of Operational Research*, 2016.
- [19] P. Belotti, J. Lee, L. Liberti, F. Margot, and A. Wachter, "Branching and bounds tighteningtechniques for non-convex minlp," *Optimization Methods Software*, vol. 24, no. 4-5, pp. 597–634, Aug. 2009. [Online]. Available: http://dx.doi.org/10.1080/10556780903087124
- [20] S. Cafieri, "Maximizing the number of solved aircraft conflicts through velocity regulation," in *MAGO 2014, 12th Global Optimization Workshop*, Málaga, Spain, Sep. 2014, pp. pp 1–4. [Online]. Available: https://hal-enac.archives-ouvertes.fr/hal-01018051
- [21] H. Hijazi, C. Coffrin, and P. V. Hentenryck, "Convex quadratic relaxations for mixed-integer nonlinear programs in power systems," *Mathematical Programming Computation*, pp. 1–47, 2016. [Online]. Available: http://dx.doi.org/10.1007/s12532-016-0112-z
- [22] C. Coffrin, H. L. Hijazi, and P. V. Hentenryck, "The QC relaxation: A theoretical and computational study on optimal power flow," *IEEE Transactions on Power Systems*, vol. 31, no. 4, pp. 3008–3018, July 2016.
- [23] H. Hijazi, "Mixed Integer NonLinear Optimization approaches for Network Design in Telecommunications," 2010, ph.D. thesis.

- [24] H. Hijazi, P. Bonami, G. Cornuéjols, and A. Ouorou, "Mixed-integer nonlinear programs featuring "on/off" constraints," *Computational Optimization and Applications*, vol. 52, no. 2, pp. 537–558, 2012.
- [25] H. L. Hijazi, P. Bonami, and A. Ouorou, "A note on linear on/off constraints," *Australian National University technical report*, 2014.
 [26] I. I. CPLEX, "V12. 1: User's manual for cplex," *International Business*
- [26] I. I. CPLEX, "V12. 1: User's manual for cplex," International Business Machines Corporation, 2009.
- [27] C. Vanaret, D. Gianazza, N. Durand, and J.-B. Gotteland, "Benchmarking conflict resolution algorithms," in 5th International Conference on Research in Air Transportation, ICRAT, Berkeley, USA, 2012, pp. 113– 114.
- [28] D. Rey, C. Rapine, V. V. Dixit, and S. T. Waller, "Equity-oriented aircraft collision avoidance model," *IEEE Transactions on Intelligent Transportation Systems*, vol. 16, no. 1, pp. 172–183, 2015.
- [29] R. Fourer, D. M. Gay, and B. W. Kernighan, AMPL: A Modeling Language for Mathematical Programming, 2nd ed. Brooks/Cole, 2002.
- [30] A. Wächter and L. T. Biegler, "On the implementation of an interiorpoint filter line-search algorithm for large-scale nonlinear programming," *Mathematical programming*, vol. 106, no. 1, pp. 25–57, 2006.
- [31] T. Lehouillier, J. Omer, F. Soumis, and G. Desaulniers, "Two decomposition algorithms for solving a minimum weight maximum clique model for the air conflict resolution problem," *European Journal of Operational Research*, vol. 256, no. 3, pp. 696–712, 2017.